agronomy

MDPI

Article

Biochar Catalysis for the Enhanced Abiotic Humification of Polyphenols: An Important Mechanism Helping Sequester Carbon

Jiangmin Zhou [1,2], Ziru Zhou [1], Chuanqing Yao [1], Yujie Zhang [1], Han Ren [1], Guining Lu [3] and Hualin Chen [1,2,*]

[1] College of Life and Environmental Sciences, Wenzhou University, Wenzhou 325035, China; rosechl@wzu.edu.cn (J.Z.); zcxzzr@126.com (Z.Z.); yyaochuanqing@163.com (C.Y.); z13215679198@163.com (Y.Z.); renhan@wzu.edu.cn (H.R.)
[2] National & Local Joint Engineering Research Center for Ecological Treatment Technology of Urban Water Pollution, Wenzhou University, Wenzhou 325035, China
[3] School of Environment and Energy, South China University of Technology, Guangzhou 510006, China; lutao@scut.edu.cn
* Correspondence: hualin2100@126.com; Tel.: +86-135-0651-0259; Fax: +86-577-86689257

Abstract: Abiotic humification, dominated by catalytic oxidation, is one of the critical mechanisms for organic carbon preservation in nature. However, the effects of biochar catalysis on abiotic humification have not yet been elucidated. This study investigated the catalytic power of biochar from walnut shells at different temperatures (300 °C, 600 °C, and 900 °C) for the abiotic transformation of hydroquinone (HQ) as a representative polyphenol. All the biochar samples catalyzed HQ polymerization, resulting in the formation of humic polymers such as fulvic acids (FAs) and humic acids (HAs). Light and oxygen promoted HA formation. $HO^{\bullet}$ was detected in the BC600–HQ reaction system, and $HO^{\bullet}$ quenching resulted in a 41.22% decrease in HA production, indicating that $HO^{\bullet}$ plays a major role in the oxidative polymerization. In the proposed pathway for the abiotic humification, biochar active sites and generated reactive oxygen species accept an electron from HQ, resulting in oxidation to (semi)quinone radicals, which subsequently undergo cleavage or a coupling reaction to form the oligomerized products. Under BC600 catalysis, the weight-average molecular weight (Mw) of the reaction products of HQ, glucose, and glycine reached 14,449 Da. These findings provide new insights into the application potential of biochar for promoting soil carbon sequestration.

Keywords: polymerization; biochar; catalytic oxidation; hydroquinone; humic substance formation

check for updates

Citation: Zhou, J.; Zhou, Z.; Yao, C.; Zhang, Y.; Ren, H.; Lu, G.; Chen, H. Biochar Catalysis for the Enhanced Abiotic Humification of Polyphenols: An Important Mechanism Helping Sequester Carbon. *Agronomy* **2024**, *14*, 1951. https://doi.org/10.3390/agronomy14091951

Academic Editor: Giovanni Gigliotti

Received: 29 July 2024
Revised: 25 August 2024
Accepted: 27 August 2024
Published: 29 August 2024

Copyright: © 2024 by the authors. Licensee MDPI, Basel, Switzerland. This article is an open access article distributed under the terms and conditions of the Creative Commons Attribution (CC BY) license (https://creativecommons.org/licenses/by/4.0/).

1. Introduction

Biochar, a carbonized solid coproduct of the thermal treatment of biomass, has attracted considerable research attention as a promising material for achieving carbon neutrality and mitigating global warming [1,2]. Biochar application can improve soil health while simultaneously suppressing CH_4 and N_2O emissions and improving soil humification [3,4]. Humification, or the formation of humic substances (HSs), is a key process in converting simple organic molecules into complex, stable, and recalcitrant macromolecules that persist in the environment over long timescales [5]. As HSs represent the largest stable organic carbon pool in terrestrial environments, enhanced humification efficiencies are vital for promoting soil carbon sequestration [6,7]. To assess the carbon sequestration potential of biochar, its effect on humification and the underlying mechanism must be clarified.

Humification processes, including the formation of fulvic acid (FA), humic acid (HA), and humin, involve a series of complex biochemical and chemical reactions such as decomposition, resynthesis, and polymerization [6,8]. In biotic humification, microorganisms decompose biological residues into low-molecular-weight substances, such as fatty acids, polyphenols, reducing sugars, and amino acids. Furthermore, through fungal extracellular

oxidative enzymes (e.g., peroxidase and laccase), microorganisms can mediate the polymerization of low-molecular-weight substances into HSs [9]. Biochar applied to soil can improve physicochemical properties such as nutrients, porosity, aeration, moisture, and pH, thus stimulating microbial activity and consequently intensifying humification [3,10].

Abiotic humification, involving abiotic or nonenzymatic reactions, is also highly efficient for HS formation in nature [11,12]. Clay minerals and metal oxides such as montmorillonite, nontronite, allophane, kaolin, zeolite, and Al, Fe, and Mn (oxyhydr)oxides can catalyze the oxidative polymerization of polyphenols [12,13], the Maillard reaction (a polymerization chain reaction between reducing sugars and free amino acids) [5,14], and the integrated polyphenol–Maillard reaction [7,15] through abiotic catalytic mechanisms. These materials can act as Lewis acids by accepting electrons from polyphenols, thereby facilitating nucleophilic addition and polycondensation reactions [16,17]. In addition, they can act as oxidants and catalysts, promoting direct oxidation, or induce reactive oxygen species (ROS) formation ($HO^{\bullet}$ and $O_2^{\bullet-}$) [7,18]. The oxidation of polyphenols or glucose generates highly reactive semiquinone radicals and carboxylic acids that readily undergo coupling reactions with other semiquinones, phenolics, amino acids, or humus [11,19].

In recent years, biochar has attracted research attention as a promising oxidant or catalyst. Notably, biochar may promote both direct and indirect catalytic oxidation in diverse chemical reactions for environmental remediation. Biochar typically contains persistent free radicals (PFRs), oxygen-containing functional groups (OFGs, e.g., quinone, ketone, carbonyl, and carboxyl), nonmetal heteroatoms, metal dopants, and graphitic structures with defects [20,21]. Owing to these intrinsic features, biochar possesses strong oxidation, electron-transfer, and catalytic abilities [22–24]. Similar to Fe and Mn (oxyhydr)oxides, biochar can act as a Lewis acid, electron acceptor, electron donor, and electron shuttle to directly participate in redox reactions [25,26]. Moreover, biochar can provide electrons to oxidants, resulting in the production of ROSs such as $HO^{\bullet}$ and $O_2^{\bullet-}$ [27]. However, to the best of our knowledge, the role of biochar catalysis in abiotic humification has yet to be investigated.

In this study, biochar prepared from walnut shells at 600 °C (BC600) was applied to the abiotic humification of polyphenols. There are various kinds of phenolic compounds in nature, like monohydric phenol, dihydric phenol, polyphenols, as well as phenol derivatives. Some phenolic compounds come from industrial wastewater, posing a serious threat to the ecosystem. Hydroquinone (HQ), a soil common low-molecular-weight phenolic compound, is mainly derived from plant polyphenols and intermediates during the microbial metabolism of anthropogenic organic compounds [28]. Furthermore, HQ has been considered as a building block for HS formation [29]. Therefore, HQ was selected as a model polyphenolic compound. The principal objectives of this study were to (1) investigate the effect of biochar on the abiotic humification reaction of HQ based on the formation of FA and HA; (2) explore the influence of factors such as light, oxygen, and biochar characteristics (as regulated by changing the pyrolysis temperature); and (3) elucidate the underlying mechanisms.

2. Materials and Methods

2.1. Reagents

HQ, sodium chloride (NaCl), sodium hydroxide (NaOH), hydrochloric acid (HCl), methanol, and 95% ethanol were purchased from Aladdin Technology Co. (Shanghai, China). Supelite™ DAX-8 resin (polymethylmethacrylate resin) (40–60 mesh) were obtained from Sigma-Aldrich Co. (Shanghai, China). Except methanol was chromatographic grade reagents, the other chemicals and reagents were analytical grade. The resistivity of deionized water used was below 18 MΩ cm^{-1}.

2.2. Biochar Preparation and Characterization

Biochar samples were produced from walnut shells at pyrolysis temperatures of 300 °C, 600 °C, and 900 °C and designated as BC300, BC600 and BC900, respectively. The detailed

preparation method referred to that of Zhou et al. [30]. The walnut shells were collected at Yunnan province in China, then washed several times with deionized water to remove the surface dirt and other impurities, and dried in an oven at 60 °C for 48 h. The dried walnut shells were smashed to pass through 0.149 mm sieve, placed in a ceramic crucible into a muffle furnace (MFLGKD408-12, Shanghai science and Technology Instrument Co., Ltd., Shanghai, China) under anaerobic atmosphere (1200 mL min^{-1} N_2). The muffle furnace was heated at a heating rate of 10 °C min^{-1} to reach a set temperature and kept for 4 h. When the pyrolytic temperature declined to room temperature under N_2 flow, the solid product (biochar) was taken out and stored in a desiccator until further use.

pH (H_2O) was determined with a mass ratio of biochar to water 1:20 using a pH Meter (FE28-standard, Mettler Toledo, Zurich, Switzerland). Dissolved organic carbon (DOC) derived from biochar was determined with a biochar to water ratio of 1:20 for complete leaching of dissolved organic matter (DOM) for 3 h in a shaker. Then, the solution was centrifuged at 3000 rpm for 15 min and the supernatant was filtered through a 0.45 μm membrane for determining total organic carbon (TOC) concentration (TOC-L CPH, Shimadzu, Hitachi, Japan). The specific surface area of biochar samples was determined at 77 K on the surface area analyzer nitrogen adsorption technology (BELSORP MAX, Osaka, Japan) according to the Brunauer–Emmett–Teller (BET) equation and the aperture distribution was analyzed by Barrett–Joyner–Halenda (BJH) method. Raman spectra were determined by a Raman spectrometer (LabRAM HR Evolution, HORIBA Scientific, Piscataway, NJ, USA) with 532 nm incident laser light. The concentration of the PFRs of biochar before and after reaction was measured by electron paramagnetic resonance (Bruker EMX PLUS, Saarbrücken, Germany). Biochar particles after reaction was filtered through 0.45 μm members (ANPEL Scientific Instrument Co., Ltd., Shanghai, China) and freeze-dried (Christ LD-1-2, Marin Christ Inc., Osterode, Germany).

2.3. Abiotic Humification Experiment

A series of the abiotic, redox-driven polymerization reactions were investigated using a batch reaction system according to Liu et al. [13]. HQ powder was dissolved and diluted with 0.5 wt.% NaCl solution, and then adjusted to pH 7.0 using a few drops of 0.1 mol L^{-1} HCl or 0.1 mol L^{-1} NaOH. A 250 mL aliquot of this solution was then transferred to a 500 mL flask and mixed with 2.5 g biochar (1% mass ratio). Our pre-experiment for dosage indicated that 1% was optimal to HA production. The flasks were shaken at 220 rpm at 25 ± 0.5 °C. Periodically, samples were sacrificed for analysis and filtered through a 0.45 μm members (ANPEL Scientific Instrument Co., Ltd., Shanghai, China). The filtrate was used for FA/HA extraction and determination. Control systems included Control 1 (0.5 wt.% NaCl solution with 1% biochar) and Control 2 (0.5 wt.% NaCl solution with HQ without biochar). The purpose of these controls was to examine the potential leaching of DOM derived from biochar and the self-oxidation of HQ.

Under dark and oxygen-poor conditions, the flasks were sealed tightly with plastic film and kept in the dark. While under light and oxygen conditions, little holes were poked the sealed plastic film for air exchange, and a 1000 W solar-simulating Xe-arc lamp (HK-1, Huikong agricultural technology Co., LTD, Weifang, China) was placed vertically on flasks.

In the $HO^{\bullet}$ quenching experiment, $HO^{\bullet}$ were removed by adding methanol (MeOH) at a concentration of 4 mol L^{-1} in the BC600-HQ system under light and oxygen conditions. The systems without MeOH were set as control.

All treatments were conducted in triplicate.

2.4. Analytical Methods

The absorbance at 400 nm (E400) and 600 nm (E600), respectively, was measured using a UV–Visible spectrophotometer (Agilent 8453, Santa Clara, CA, USA). Before the absorbance measurements, the pH of the sample solution was adjusted to 7.0 by 0.1 mol L^{-1} HCl and NaOH. The pH value of the reaction system was examine using a pH meter (FE28-standard, Mettler Toledo, Zurich, Switzerland). The concentration of DOC was determined

with TOC analyzer (TOC-L CPH, Shimadzu, Hitachi, Japan). The concentration of HQ was quantified with a high-performance liquid chromatography (HPLC) instrument equipped with a diode array detector (DAD; Agilent 1260, Santa Clara, CA, USA). Methanol and water (60:40) were used as the mobile phase at a flow rate of 0.4 mL min^{-1}. The injection volume was 10 μL, and the UV detector was set at 270 nm. The extraction of fulvic acids (FAs) and humic acids (HAs) was conducted according to the International Humic Substances Society (IHSS) standard protocol [12]. The concentrations of extracted HAs and FAs were measured by TOC analyzer.

The $HO^{\bullet}$ generation in the BC600–HQ system was investigated using a spin-trapping agent (5,5-dimethyl-1-pyrrole-N-oxide, DMPO). At the scheduled reaction time (72 h), 1 mL of the mixture was withdrawn from the suspension of BC600–HQ system and was filtered using a 0.45-μm membrane. Then, 2 mL of DMPO solution (50 m mol L^{-1}) was immediately mixed with the filtered sample for 1 min. Then, the mixture was loaded in quartz capillary tubes for EPR analysis.

The main polymerization products in the BC600–HQ system were analyzed using GC–MS. After filtration (0.45 μm), the supernatant was placed in a 2 mL ampere flask and dried under nitrogen flow. The dried powder was redissolved in methylene chloride, then transferred to 150 μL insert vials and analyzed by GC–MS (Agilent 7890A-5975C, Santa Clara, CA, USA). The products detected in the reaction systems were identified using NIST 17. Library or speculated products based on molecule weight calculations.

The molecular weight (Mw) of the reaction mixture was measured by high-performance liquid chromatography-size exclusion chromatography (HPLC-SEC), carried out on HPLC-DAD (Agilent 1260, Santa Clara, CA, USA).

2.5. Statistical Analysis

IBM SPSS 19.0 software was used to implement the statistical analysis of the experimental data. Data were graphed using Origin Pro 2020 (OriginLab, Northampton, MA, USA).

3. Results and Discussion

3.1. Humification Process and HQ Transformation under BC600 Catalysis

Previous studies have shown that biochar prepared at 600 °C had the strongest PFRs [21]. So, BC600 was used as an example to investigate the humification process of HQ under oxygen-poor and dark conditions. As the reaction time increased, the solution changed from colorless to deep brown in the BC600–HQ system, whereas almost no change occurred in the control system with only BC600 or HQ. The absorbance of the supernatant at 400 nm (E_{400}) was used to monitor the formation of colored substances and thus indicate the degree of humification [7]. In the BC600–HQ system, E_{400} increased dramatically over the first 144 h, with subsequent sluggish growth until the end of the reaction (Figure 1C). Moreover, the HQ content of the BC600–HQ system decreased rapidly (Figure 1A). After 7 h of reaction, the dissolved organic carbon (DOC) content in the solution was far greater than the carbon content of HQ, as calculated using its molecular formula (Figure 1A,B). At the end of reaction, the carbon content of HQ was approximately one-tenth of the DOC content in solution. Therefore, the decrease in HQ in the BC600–HQ system was mainly due to the chemical transformation of HQ into brown substances.

Because the control systems did not exhibit obvious changes in color or absorbance and no precipitation occurred during the reaction pH 2, we did not analyze the E_{400}/E_{600} ratio, FA, or HA in the control systems. In the BC600–HQ system, the FA content first increased sharply and then decreased until a dynamic balance was achieved. In contrast, the HA content initially increased quickly in the beginning before increasing more slowly until the end of the reaction (Figure 1F). The corresponding decrease in pH further confirmed the generation of FA and HA (Figure 1E). Based on these trends, FA was generated at the beginning of the reaction and rapidly converted into HA, which is consistent with other biotic and abiotic humification processes [31,32]. According to Zhang et al. [32],

the humification process can be divided into two steps. First, small molecules of organic matter formed FAs. Second, FAs were rapidly converted to HAs. In this study, HQ generated FAs at the beginning of the reaction, and most FAs were converted into HAs. After 144 h of reaction, some FAs formed short-life intermediates (converted into HAs), other FAs formed unstable substances that can be decomposed with releasing carbon dioxide, and the remaining FAs were in a dynamic equilibrium [32]. Correspondingly, HA content increased slowly during the later stage of reaction. In addition, the E_{400}/E_{600} ratio decreased over time (Figure 1D), indicating that the molecular weight and degree of reaction product condensation increased as the reaction processed in the BC600–HQ system [33]. These results demonstrated that the presence of BC600 significantly enhanced the abiotic humification of HQ.

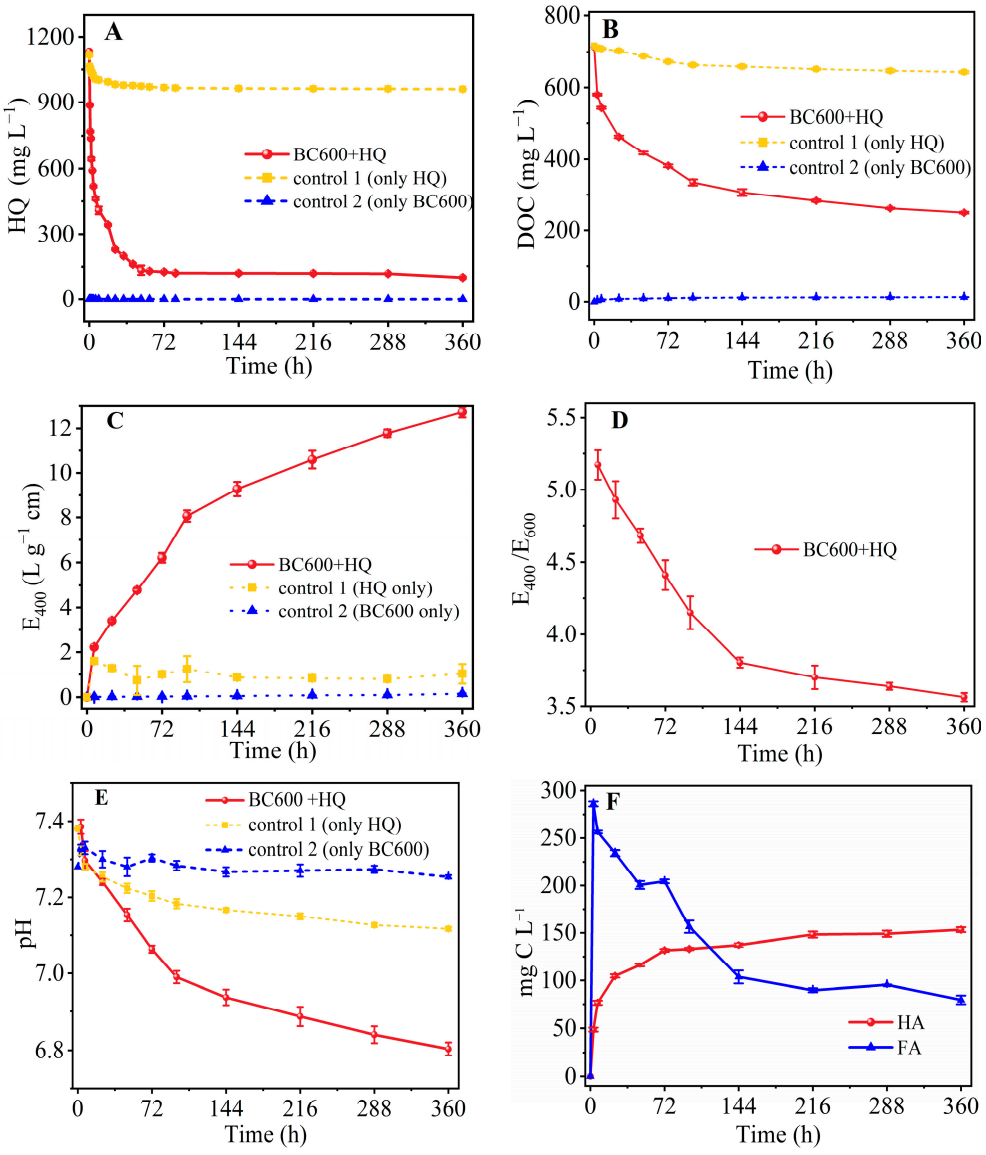


Figure 1. Changes in BC600–HQ system during the 360 h reaction under dark and oxygen-poor conditions. ((**A**) HQ concentration, (**B**) DOC concentration, (**C**) UV–Vis absorbance value at 400 nm, (**D**) ratio of UV–Vis absorbance value at 400 nm and 600 nm, (**E**) pH value, (**F**) FA and HA concentration).

Previous studies have reported that biochar contains highly active OFGs (e.g., hydroxyl and carboxyl groups), PFRs, and transition metals (e.g., iron and cobalt) that can accept and donate electrons, mediate electron transfer, and induce free radical reactions [22,24]. The OFGs of BC600 can act as Lewis acid sites to accept electrons from HQ, resulting in the generation of semiquinone radical and phenoxy radicals [34]. Moreover, in an aquatic environment, BC600 can react with water to generate various ROSs (such as $HO^{\bullet}$ and $O_2^{\bullet-}$) [27]. Under catalysis by PFRs in BC600 and the produced ROSs, HQ was oxidized and degraded to form various intermediate products, including *p*-benzoquinone, semiquinone radicals, phenoxy radicals, and small organic acid (e.g., fumaric acid, maleic acid, and oxalic acid) [28,35,36]. These species can undergo polymerization via a series of oxidation coupling reactions, resulting in the formation of dark-colored humic analogs (FA and HA) [37]. Liu et al. [13] reported that hexagonal and triclinic birnessites (δ-MnO_2) catalyze the formation of HA from HQ via coupling, cleavage, polymerization, and decarboxylation reactions. Dou et al. [20] demonstrated that various phenolic substances in a biochar-activated peroxydisulfate system can generate dimeric and oligomeric substances through coupling and polymerization reactions. Gokturk et al. [38] showed that HQ polymers with the molecular weights up to 11.6×10^3 g mol^{-1} are produced via oxidation and free-radical reactions catalyzed by hybrid nanoflowers. As observed by Zhang et al. [35], phenolic compounds undergo polymerization and degradation simultaneously during the free radical reactions in supercritical water; however, upon increasing the oxidant equivalent, all the intermediate products gradually degraded into CO_2 and H_2O. In the BC600-HQ system, the HQ content decreased sharply over the first 5 h and more slowly until the end of reaction, which was ascribed to the synergistic effect of the adsorption, oxidation, polymerization, and mineralization of HQ [39].

3.2. Impact of Light and Oxygen

Previous studies have demonstrated that light irradiation and molecular oxygen (O_2) exert an important impact on biochar's catalytic efficiency, since light irradiation and O_2 can trigger the generation of free radicals and ROSs [22,26]. Therefore, the effects of light irradiation and O_2 on abiotic polymerization was investigated, using a system with 0.2 mol L^{-1} HQ as an example. In the presence of light and O_2, the DOC content decreased more rapidly than under dark and oxygen-poor conditions (Figure 2A), consistent with the results reported by Velasco et al. [39]. Under both conditions, a similar amount of DOC was adsorbed on BC600. Therefore, light and O_2 promoted the complete degradation of HQ into CO_2 via a photo-oxidation process, thereby decreasing the DOC content in the solution. Moreover, the pH was lower and HA concentration increased greatly (by 47.50%) in the presence of light and O_2 compared with that under dark and oxygen-poor conditions (Figure 2B,D). These results verified that HA synthesis and HQ degradation occurred simultaneously during abiotic humification, which is consistent with previous studies that carbon release was positively correlated with the HA yield [9]. Under light irradiation and O_2 exposure, the BC600 surface produced more PFRs [23]. Additionally, HQ and its intermediate degradation products include various types of light-absorbing DOM, such as phenolic, semiquinone, and quinone groups, which can be excited to an excited state (^{1}DOM* and ^{3}DOM*) under light irradiation and then transformed into $DOM^{+\bullet}$ and $DOM^{-\bullet}$ through intramolecular electron transfer [40]. When O_2 is abundant, reactions with PFRs and excited-state DOM (^{1}DOM* and ^{3}DOM*) can induce $HO^{\bullet}$, $O_2^{\bullet-}$, $^1O_2$, and H_2O_2 formation [41], thereby increasing the oxidation performance of the BC600–HQ system to promote oxidation, degradation, cross-coupling, and polymerization reactions [39,42].

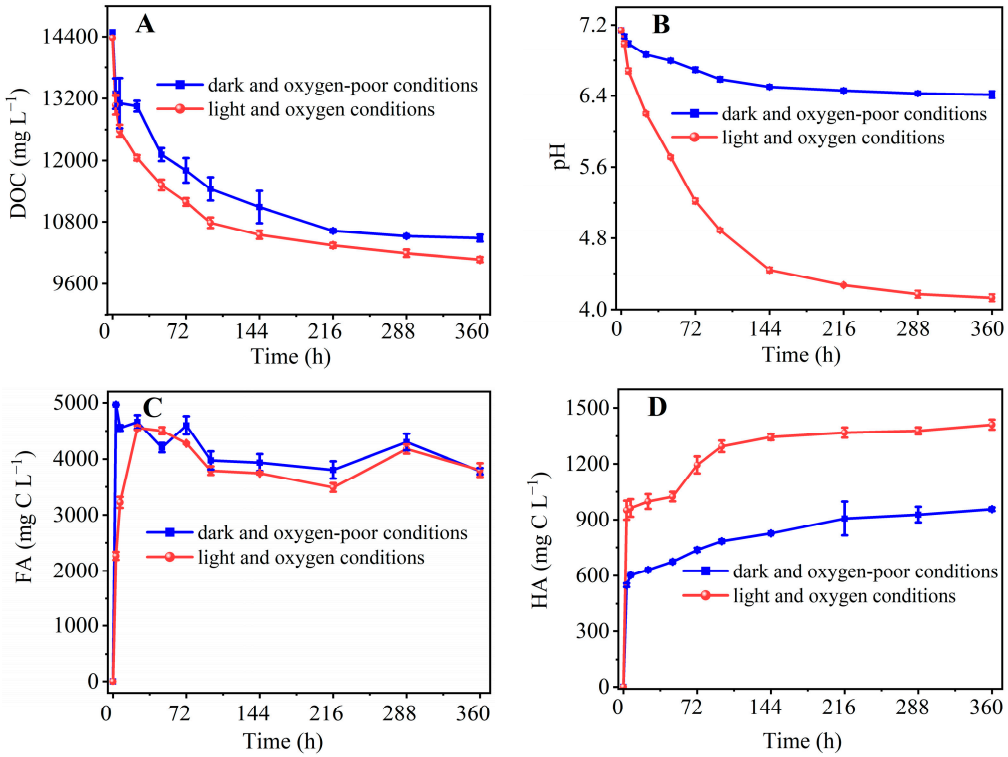


Figure 2. Impact of light and oxygen on abiotic humification during the 360 h reaction. ((**A**) DOC concentration. (**B**) pH value. (**C**) FA concentration. (**D**) HA concentration).

3.3. HO• Quenching Experiment under Light and O_2 Conditions

HO• has been widely reported to be a key ROS in biochar catalysis applications. As HO• can attack aromatic carbon to promote aromatic ring opening, this species plays an essential role in the removal of recalcitrant organic pollutants, organic carbon oxidation in soil, and the oxidative polycondensation of phenolic and amino acids [22,23,43]. In this study, the presence of HO• in the BC600–HQ system under light and O_2 conditions was investigated using spin-trapping electron paramagnetic resonance (EPR) and quenching experiments. Distinct signals corresponding of 5,5-dimethyl-1-pyrroline *N*-oxide (DMPO)−HO• (1:2:2:1) adducts in the BC600–HQ systems confirmed the formation of HO• (Figure 3A).

Methanol (MeOH) quenching experiments were performed to investigate the effect of HO• on abiotic polymerization in the BC600–HQ system. As shown in Figure 3C,D,E, MeOH addition decreased the FA and HA contents and increased the pH after 360 h of reaction. The FA and HA content in the presence of MeOH were 35% and 59% of those in the absence of MeOH, suggesting that HO• contributed to the abiotic polymerization of HQ. The initial DOC concentration in the presence of MeOH was significantly higher than that in the absence of MeOH because of excess organic C from MeOH (Figure 3B). After the 360 h reaction, the DOC content decreased to a greater extent in the presence of MeOH (41% vs. 30%), which was mainly attributed to the loss of CO_2 by the reaction between MeOH and HO• [44].

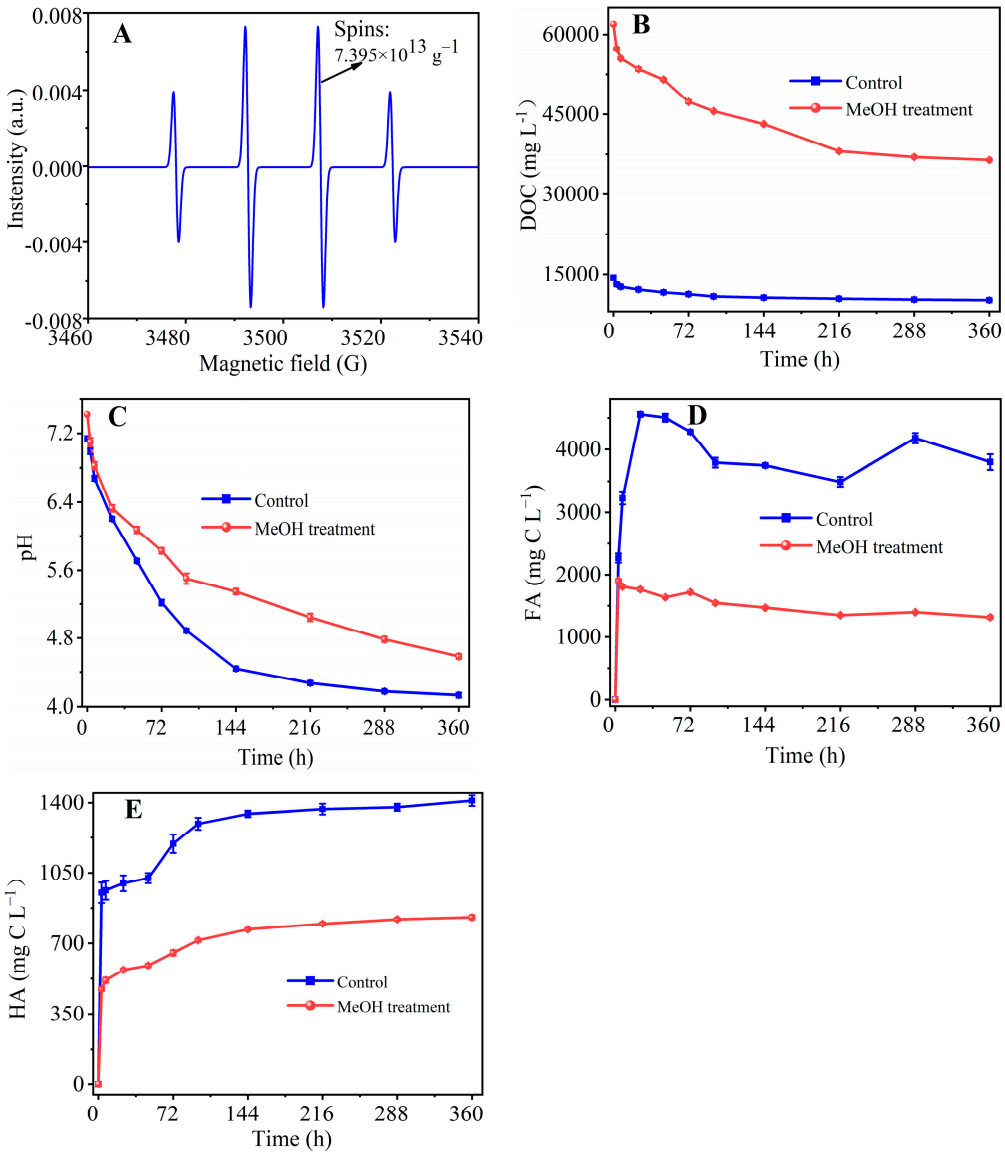


Figure 3. HO• detection with DMPO as the spin-trapping agent and HO• quenching experiment in the BC600–HQ system during the 360 h reaction. ((**A**) EPR spectra of DMPO-HO• adduct, (**B**) DOC concentration, (**C**) pH value, (**D**) FA concentration, (**E**) HA concentration).

3.4. Effect of Pyrolysis Temperature on Biochar Performance

To verify the catalytic power of biochar for the abiotic polymerization of HQ, BC300 and BC900 were prepared and compared with BC600. Similar to BC600, BC300 and BC900 promoted HQ polymerization (Figure 4A). Based on the HA content, BC600 and BC900 exhibited similar catalytic performance for HQ polymerization, whereas the performance of BC300 was inferior. This trend is in agreement with previous studies, in which the catalytic activity of biochar was found to be affected by the pyrolysis temperature [20,25]. The active moieties in biochar have been reported to include biochar-derived dissolved organic matters (BDOM), OFGs, PFRs, nonmetal heteroatoms, metal dopants, graphitization structure, and defects [24]. In this study, BC300 contained the most BDOM (Table 1) and some PFRs (Figure 4B), whereas BC600 contained the highest concentration of PFRs (2.79×10^{15} spins g^{-1}). Because most unstable compounds in the feedstocks were decomposed or transformed at high pyrolysis temperature [45], BC900 contained little BDOM, few OFGs, and no PFRs. However, the high pyrolysis temperature caused BC900 to have the most defects in the carbon lattice, as confirmed by the high I_D/I_G value by using the in-

tensity of D band (1350 cm^{-1}) and G band (1610 cm^{-1}) in Raman spectroscopy (Figure 4C). The defects in the carbon lattice may be the main active sites in BC900. These defects could shift the charge density of HQ to form an electron-deficient activated state (HQ*), which could undergo electrochemical polymerization [20]. Additionally, the dangling σ bonds of the defects could release π-electrons from the conjugated network, promoting electron transfer from BC900 to O_2 and the generation of ROSs [24]. At the end of reaction, the filtered biochar particles were collected, freeze-dried, and analyzed by EPR to quantify the PFR concentrations. Intriguingly, the PFR concentrations on BC300, BC600 and BC900 increased significantly after the reaction (Figure 4D), which might be due to the sorption of generated organic free radicals, such as phenoxyl and alkoxyl radicals, by the biochar during reaction process [46], further demonstrating that the radical chain reactions are essential for HA formation.

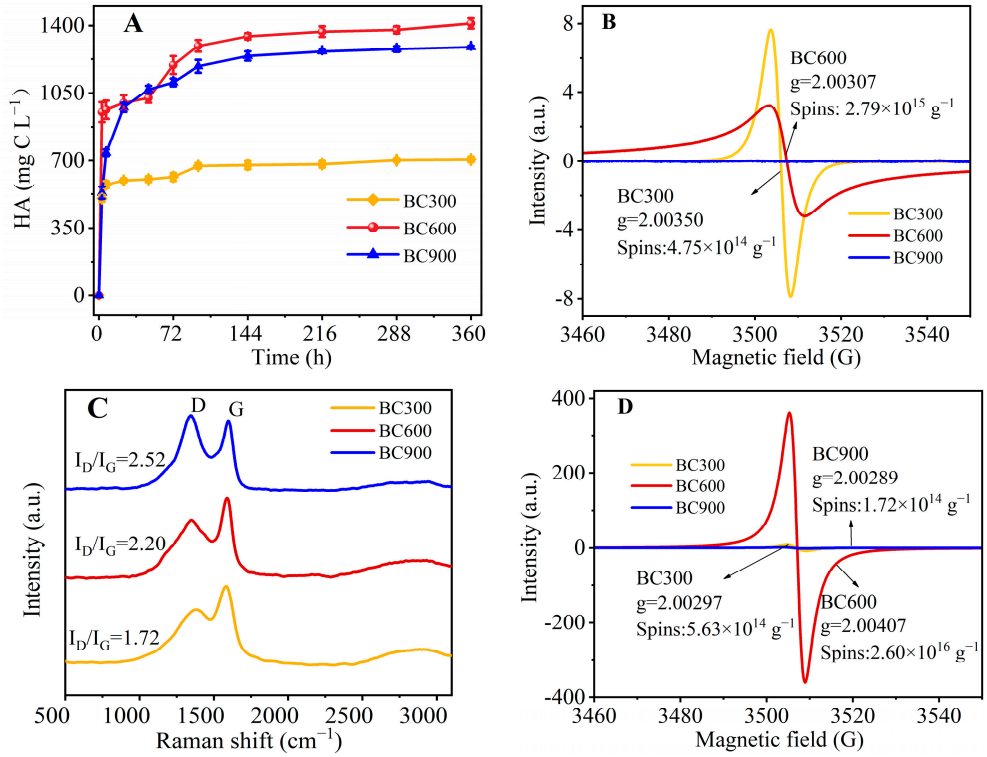


Figure 4. (**A**) Comparison of HA concentration catalyzed by biochar prepared at 300 °C (BC300), 600 °C (BC600), and 900 °C (BC900). (**B**) Persistent free radicals (PFRs) of BC300, BC600, and BC900 before reaction. (**C**) Raman spectra of BC300, BC600, and BC900. (**D**) PFRs of BC300, BC600, and BC900 after reaction.

Table 1. Properties of biochar produced in different pyrolysis temperatures.

Biochar	Yield [a] (%)	pH	DOC (mg g^{-1})	S_{BET} [b] (m^2 g^{-1})	S_{micro} [c] (m^2 g^{-1})	V_{total} [d] (cm^3 g^{-1})	V_{micro} [e] (cm^3 g^{-1})
BC300	40.89	7.38	0.74	6.77	4.69	0.005	0.002
BC600	24.56	11.47	0.28	329.51	303.04	0.14	0.11
BC900	23.21	12.02	0.05	26.69	27.52	0.02	0.01

Note: [a] rate of biochar from pyrolysis of raw material, [b] S_{BET} specific surface area, [c] S_{micro} micropore surface area, [d] V_{total} total volume, [e] V_{micro} micropore volume.

3.5. Transformation Products and Proposed Reaction Pathway for the Abiotic Humification Reaction of HQ over BC600

To determine the reaction pathway of HQ polymerization during the catalytic process over BC600, GC-MS was employed to investigate the transformation products after 24, 128,

and 360 h. To exclude the DOM derived from BC600, BC600 alone was evaluated after 360 h as a control system. The total ion chromatograms (TICs) at various reaction stages and compounds identified using NIST library are shown in Figure 5 and Table S1, respectively. Compared with the control system, more transformation products were detected in the BC600–HQ system. The content of HQ [(RT (Retention Time) = 11.26 min)] decreased with increasing reaction time. The predominant reaction products in the BC600–HQ system were *p*-benzoquinone [RT = 6.65 min, 24 h (reaction time in the BC600–HQ system)], resorcinol (RT = 11.92 min, 128 h), 2-ethylbutyl methyl phthalate (RT = 14.00 min, 128 h), long-chain fatty acids (RT = 27.02 min, 128 h), 1,2,4-Benzenetricarboxylic acid 4-dodecyl 1,2-dimethyl ester (RT = 34.91 min, 24 h), and some complex polymers. The structural subunits of HA can be considered as methylated phenol derivatives [7]. Although some methylated phenol derivatives, such as 2,6-bis(1,1-dimethylethyl)-phenol, were detected in the control system, these compounds were richer and more complex in the BC600–HQ system. Because of its high activity after light absorption [46], some BC600-derived DOM participated in the polymerization reaction of HQ. The appearance of diisooctyl phthalate (RT = 28.66 min, 24 h) and 2-ethylbutyl methyl phthalate (RT = 14.00 min, 128 h) indicated that HSs were formed rapidly from the oxidative polymerization of HQ and BC600-derived DOM in the BC600–HQ system. As the reaction time increased, the amount of long-chain products increased, the alkyl chain length increased, and a prominent peak at 28.59 min (1,1′,1″,1‴-(1,5-hexadiene-1,3,4,6-tetrayl) tetrakis-Benzene) was presented in the 360 h sample, demonstrating the accumulation of more complex polymerization products with longer RT.

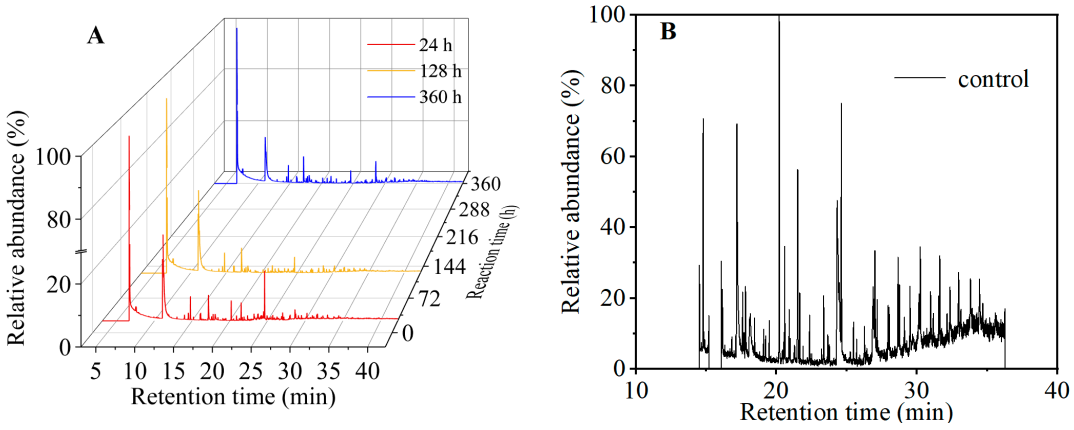


Figure 5. Total ion chromatogram (TIC) of GC–MS for (**A**) BC600–HQ reaction system and (**B**) control system (only BC600).

Based on these transformation products, four routes were proposed for abiotic humification of HQ over BC600 (Figure 6):

(I). HQ is rapidly oxidized to semiquinones or *p*-benzoquinone radicals by BC600 and ROS like HO•. On the one hand, the configurational transition of *p*-benzoquinone radicals generates *p*-benzoquinone (RT = 6.65 min, 24 h) [13,47]. Subsequently, some *p*-benzoquinone is oxidized by HO• to break the C–C single bond between the C=O and C=C double bond [48], leading to ring cleavage of *p*-benzoquinone and formation of carboxylic acid fragments and alkenes. Some small carboxylic acid molecules are degraded into inorganic molecules such as CO_2 and H_2O [36]. On the other hand, *p*-benzoquinone radicals undergo a series of oxidation coupling reactions to form oligomers, such as 5,6,12,13-tetrahydro- Dibenz[a,h]anthracene (RT = 34.90 min, 128 h) [7,20].

(II). The polymerization of benzoquinone, carboxylic acid fragments, and alkenes via Diels–Alder reaction, esterification, and cyclization reaction produces HSs, including 2-(1,3-cyclohexadienyl)-5,5-dimethyl-1,3-Cyclohexanedione (RT = 16.7 min, 24 h),

1,2,4-Benzenetricarboxylic acid 4-dodecyl 1,2-dimethyl ester (RT = 34.91 min, 24 h), 1,3-Benzenedicarboxylic acid, bis(2-ethylhexyl) ester (RT = 30.72 min, 128 h), 7,9-Di-tert-butyl-1-oxaspiro(4,5)deca-6,9-diene-2,8-dione (RT = 20.97 min, 360 h), and 1,1′,1″,1‴-(1,5-hexadiene-1,3,4,6-tetrayl) tetrakis- Benzene (RT = 28.59 min, 360 h).

(III). HSs are produced by the polymerization of BC600-derived DOM, carboxylic acid fragments, and alkenes. Dibutyl phthalate (RT = 21.51 min, control), generated by BC600 and alkenes, undergoes addition reactions to form diisooctyl phthalate (RT = 28.66 min, 24 h) and 2-ethylbutyl methyl phthalate (RT = 14.00 min, 128 h). Heptadecyl acetate (RT = 27.02 min, 128 h) and tricosyl acetate (RT = 24.62, 360 h) may originate from hexadecane (RT = 16.07 min, control) and 1-Octadecene (RT = 24.63 min, control) from BC600.

(IV). HSs such as phthalic acid and isobutyl 2-methylpent-3-yl ester originate from BC600, as these compounds were detected in both the control system and the BC600–HQ systems.

HPLC-SEC was used to determine the molecular weight (Mw) of the oxidative polymerization products of HQ produced over BC600 under light and oxygen conditions. After 360 h of reaction, the weight-averaged Mw value of the reaction products for HQ alone was 463 Da (Table 2), which was much lower than that obtained by catalysis with MnO_2. However, the polyphenol–Maillard reaction (HQ + glucose + glycine) over BC600 generated products with weight-averaged Mw values of 8143 Da and 14,449 Da, respectively, which are comparable to the Mw of soil-derived HA [49]. These results further demonstrate that biochar promoted abiotic humification.

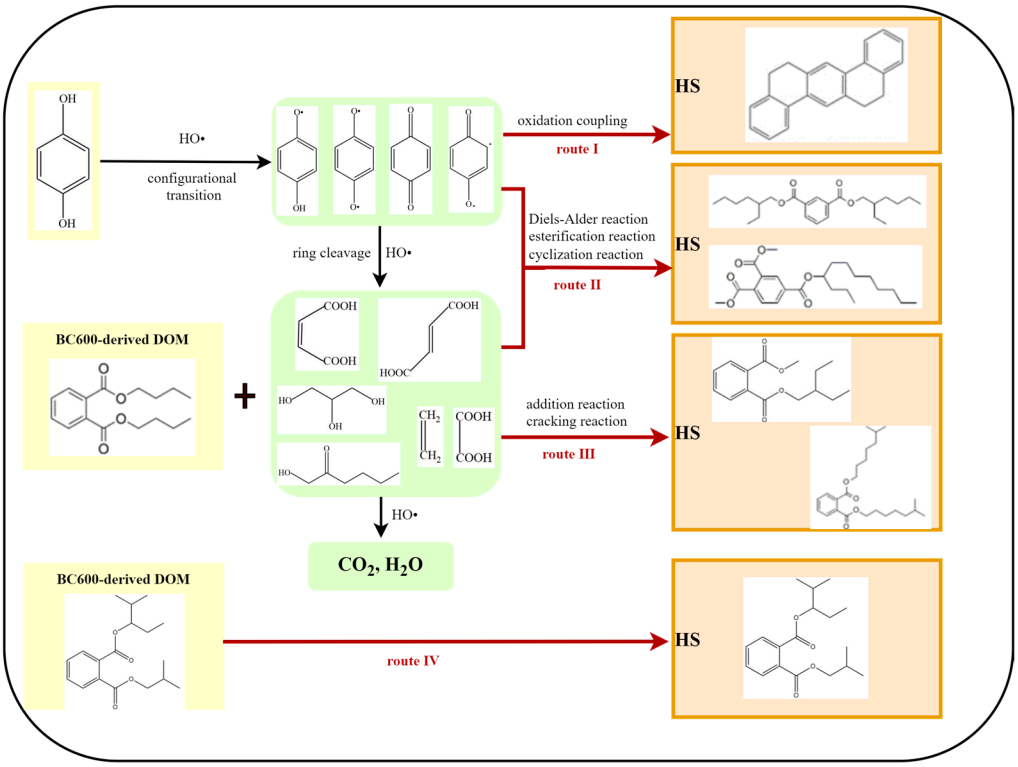


Figure 6. Graphical scheme for proposed route of HQ abiotic humification reaction under BC600 catalysis.

Table 2. Molecular weight of humification products catalyzed by BC600.

Sample	Mn [a] (Da)	Mw [b] (Da)	Mp [c] (Da)	Mz [d] (Da)	Polydispersity
only HQ	420	463	407	516	1.103
HQ + glucose	13,935	14,449	12,668	15,193	1.037
+ glycine	8033	8143	8487	8234	1.014

Note: [a] number-average molecular weight; [b] weight-average molecular weight; [c] peak molecular weight; [d] Z-average molecular weight.

4. Conclusions and Implications

Biochar produced from walnut shells at different temperatures all significantly enhanced the abiotic humification through the oxidative polymerization of HQ, as demonstrated by an increase in E_{400}, a decrease in pH, and the formation of FAs and HAs. Light and oxygen were conducive to HA formation. The presence of HO$^{\bullet}$ in the BC600–HQ system under light and oxygen conditions was verified using the DMPO trapping technique. HO$^{\bullet}$ quenching led to a decrease in the contents of FA and HA, suggesting that HO$^{\bullet}$ plays an important role in the oxidative polymerization of HQ. BC600 and BC900 exhibited a similar catalytic performance for HA formation, whereas the performance of BC300 was inferior. The following routes for abiotic humification were proposed: The active sites of biochar, such as OFGs, PFRs, defects in graphitic domains, and generated ROS (HO$^{\bullet}$) accept an electron from HQ, which is oxidized to (semi)quinone radicals. Subsequently, the coupling of these (semi)quinone radicals can lead to the formation of HS. In addition, the degradation of these (semi)quinone radicals can release CO_2, carboxylic acid fragments, and alkenes, which can polymerize to form HSs. Biochar-derived DOM may be involved in HS formation, either directly or through polymerization with the degradation products of (semi)quinone radicals.

The remarkable promoting effects of biochar on the synthesis of HSs suggest that the role of this material on soil carbon sequestration and composting process should be considered. These findings emphasize the significance of biochar's catalytic ability and demonstrate the key mechanism of biochar in the formation of HSs, offering valuable insights for biochar soil application as a negative emission technology. It is also a novel method to recycle phenolic compounds from wastewater through chemical catalytic humification. However, it should be noted that, upon applying biochar to soils, the PFRs of biochar and ROS formation may be activated or inactivated by ions, natural organic matter, and clay particles, depending on the soil properties. The reported decrease in the HS content of some soils after biochar application most likely results from an enhancement of the mineralization process of native organic compounds by the PFRs of biochar and HO$^{\bullet}$. Therefore, further investigation is required to clarify the dynamic of PFRs and their influence on organic carbon transformation in soil. Meanwhile, further investigation on the relationship among biochar characteristics, catalytic ability, and polymerization reaction is essential.

Supplementary Materials: The following supporting information can be downloaded at: https://www.mdpi.com/article/10.3390/agronomy14091951/s1, Table S1: Some transformation products identified by GC-MS analysis and NIST library matching.

Author Contributions: Conceptualization, J.Z.; Data curation, J.Z.; Formal analysis, J.Z.; Funding acquisition, H.C.; Investigation, Z.Z., C.Y. and Y.Z.; Methodology, J.Z. and G.L.; Project administration, H.C.; Validation, H.R.; Writing—original draft, J.Z. All authors have read and agreed to the published version of the manuscript.

Funding: This research was funded by the Science and Technology Department of Zhejiang Province (Project No. 2019C54002).

Data Availability Statement: The original contributions presented in the study are included in the article/Supplementary Materials; further inquiries can be directed to the corresponding author.

Conflicts of Interest: The authors declare no conflict of interest.

References

1. Deng, X.; Teng, F.; Chen, M.P.; Du, Z.L.; Wang, B.; Li, R.Q.; Wang, P. Exploring negative emission potential of biochar to achieve carbon neutrality goal in China. *Nat. Commun.* **2024**, *15*, 1085. [CrossRef] [PubMed]
2. Lehmann, J.; Cowie, A.; Masiello, C.A.; Kammann, C.; Woolf, D.; Amonette, J.E.; Cayuela, M.L.; Camps-Arbestain, M.; Whitman, T. Biochar in climate change mitigation. *Nat. Geosci.* **2021**, *12*, 883–892. [CrossRef]
3. Cybulak, M.; Sokołowska, Z.; Boguta, P. The influence of biochar on the content of carbon and the chemical transformations of fallow and grassland humic acids. *Sci. Rep.* **2021**, *11*, 5698. [CrossRef]
4. Wang, L.W.; Deng, J.Y.; Yang, X.D.; Hou, R.J.; Hou, D.Y. Role of biochar toward carbon neutrality. *Carbon Res.* **2023**, *2*, 2. [CrossRef]
5. Moore, O.W.; Curti, L.; Woulds, C.; Bradley, J.A.; Babakhani, P.; Mills, B.J.W.; Homoky, W.B.; Xiao, K.Q.; Bray, A.W.; Fisher, B.J.; et al. Long-term organic carbon preservation enhanced by iron and manganese. *Nature* **2023**, *621*, 312–317. [CrossRef] [PubMed]
6. Dou, S.; Shan, J.; Song, X.Y.; Cao, R.; Wu, M.; Li, C.L.; Guan, S. Are humic substances soil microbial residues or unique synthesized compounds? A perspective on their distinctiveness. *Pedosphere* **2020**, *2*, 159–167. [CrossRef]
7. Zhang, X.M.; Zong, Y.; Xu, L.Q.; Mao, Y.F.; Wu, D.L. Enhanced abiotic integrated polyphenol-Maillard humification by Mg/Fe layered double hydroxide (LDH): Role of Fe(III)-polyphenol complexation. *Chem. Eng. J.* **2021**, *425*, 130521. [CrossRef]
8. Zavarzina, A.G.; Danchenko, N.N.; Demin, V.V.; Artemyevas, Z.S.; Kogut, B.M. Humic Substances: Hypotheses and Reality (a Review). *Eurasian Soil Sci.* **2021**, *54*, 1826–1854. [CrossRef]
9. Zhang, Y.C.; Xu, Y.; Yu, X.L.; Li, J.K.; Chen, G.; Wang, S.J.; Xu, Y.P.; Xu, R.; Zhang, B.H.; Zhang, H.Q. Microbial metabolism and humic acid formation in response to enhanced copper and zinc passivation during composting of wine grape pomace and pig manure. *Bioresour. Technol.* **2023**, *384*, 129226. [CrossRef]
10. Meng, W.S.; Zhu, F.N.; Wang, X.R.; Guan, S.; Dou, S.; Ndzelu, B.S. Contrasting effects of straw and straw-derived biochar application on soil organic matter and corn yield in a Chinese Mollisol. *J. Soil. Sediment.* **2023**, *23*, 3843–3856. [CrossRef]
11. Zhang, Y.C.; Bi, Z.T.; Tian, W.X.; Ge, Z.Y.; Xu, Y.; Xu, R.; Zhang, H.Q.; Tang, S.F. Synergistic effect triggered by Fe_2O_3 and oxygen-induced hydroxyl radical enhances formation of amino-phenolic humic-like substance. *J. Environ. Manag.* **2023**, *348*, 119312. [CrossRef] [PubMed]
12. Zou, J.; Huang, J.Z.; Yue, D.B.; Zhang, H.C. Roles of oxygen and Mn (IV) oxide in abiotic formation of humic substances by oxidative polymerization of polyphenol and amino acid. *Chem. Eng. J.* **2020**, *393*, 124734. [CrossRef]
13. Liu, M.M.; Cao, X.H.; Tan, W.F.; Feng, X.H.; Qiu, G.H.; Chen, X.H.; Liu, F. Structural controls on the catalytic polymerization of hydroquinone by birnessites. *Clays Clay Miner.* **2011**, *5*, 525–537. [CrossRef]
14. Jokic, A.; Frenkel, A.; Vairavamurthy, M.; Huang, P. Birnessite catalysis of the Maillard reaction: Its significance in natural humification. *Geophys. Res. Lett.* **2001**, *28*, 3899–3902. [CrossRef]
15. Wang, M.C.; Huang, P.M. Cleavage of ^{14}C-labeled glycine and its polycondensation with pyrogallol as catalyzed by birnessite. *Geoderma* **2005**, *124*, 415–426. [CrossRef]
16. Hardie, A.G.; Dynes, J.J.; Kozak, L.M.; Huang, P.M. Influence of polyphenols on the integrated polyphenol-maillard reaction humification pathway as catalyzed by birnessite. *Ann. Environ. Sci.* **2007**, *1*, 91–110.
17. Miura, A.; Okabe, R.; Izumo, K.; Fukushima, M. Influence of the physicochemical properties of clay minerals on the degree of darkening via polycondensation reactions between catechol and glycine. *Appl. Clay Sci.* **2009**, *46*, 277–282. [CrossRef]
18. Bui, V.K.H.; Nguyen, X.C.; Bang, T.H.; Jin, H. Using CuMgFe layered double oxide to replace laccase as a catalyst for abiotic humification. *Chemosphere* **2024**, *353*, 141647. [CrossRef]
19. Zhang, Y.C.; Yue, D.B.; Fang, D.; Dong, X.W.; Li, W.L. Enhanced darkening effect from the interaction of MnO_2 and oxygen on the component evolution of amino-phenolic humic-like substances. *Chemosphere* **2021**, *263*, 127956. [CrossRef]
20. Dou, J.B.; Tang, Y.; Lu, Z.J.; He, G.Z.; Xu, J.M.; He, Y. Neglected but efficient electron utilization driven by biochar-coactivated phenols and peroxydisulfate: Polyphenol accumulation rather than mineralization. *Environ. Sci. Technol.* **2023**, *14*, 5703–5713. [CrossRef]
21. Lyu, H.H.; Zhang, Q.R.; Shen, B.X. Application of biochar and its composites in catalysis. *Chemosphere* **2020**, *240*, 124842. [CrossRef] [PubMed]
22. Fang, G.D.; Zhu, C.Y.; Dionysiou, D.D.; Gao, J.; Zhou, D.M. Mechanism of hydroxyl radical generation from biochar suspensions: Implications to diethyl phthalate degradation. *Bioresour. Technol.* **2015**, *176*, 210–217. [CrossRef] [PubMed]
23. Fang, G.D.; Liu, C.; Wang, Y.J.; Dionysiou, D.D.; Zhou, D.M. Photogeneration of reactive oxygen species from biochar suspension for diethyl phthalate degradation. *Appl. Catal. B Environ.* **2017**, *214*, 34–45. [CrossRef]
24. Gao, Y.; Sun, Y.R.; Song, W.S.; Jia, Y.F.; Li, A.M.; Wang, S.F. Intrinsic properties of biochar for electron transfer. *Chem. Eng. J.* **2023**, *475*, 146356. [CrossRef]
25. Baye, F.A.; Bandal, H.A.; Kim, H. FeCx-coated biochar nanosheets as efficient bifunctional catalyst for electrochemical detection and reduction of 4-nitrophenol. *Environ. Res.* **2024**, *246*, 118071. [CrossRef]
26. Zhang, P.; Zhang, P.J.; Feng, S.H.; Li, H.; Li, J.; Du, W.; Duan, W.Y.; Li, X.H.; Zhang, C.; Li, H.X.; et al. The mechanism of p-nitrophenol degradation by dissolved organic matter derived from biochar. *Sci. Total Environ.* **2023**, *868*, 8. [CrossRef]
27. Zhang, R.R.; Zhang, R.L.; Zimmerman, A.R.; Wang, H.L.; Gao, B. Applications, impacts, and management of biochar persistent free radicals: A review. *Environ. Pollut.* **2023**, *15*, 121543. [CrossRef]

28. Sun, Z.Y.; Chu, L.G.; Wang, X.H.; Fang, G.D.; Liu, C.; Chen, H.; Gu, C.; Gao, J. Roles of natural phenolic compounds in polycyclic aromatic hydrocarbons abiotic attenuation at soil-air interfaces through oxidative coupling reactions. *Environ. Sci. Technol.* **2023**, *32*, 11967–11976. [CrossRef]
29. Qin, W.X.; Wang, Y.J.; Fang, G.D.; Liu, C.; Sui, Y.X.; Zhou, D.M. Oxidation mechanism of As(III) in the presence of polyphenols: New insights into the reactive oxygen species. *Chem. Eng. J.* **2016**, *285*, 69–76. [CrossRef]
30. Zhou, J.M.; Chen, H.L.; Tao, Y.L.; Thring, R.W.; Mao, J.L. Biochar amendment of chromium-polluted paddy soil suppresses greenhouse gas emissions and decreases chromium uptake by rice grain. *J. Soil Sediment.* **2019**, *19*, 1756–1766. [CrossRef]
31. Duan, Y.M.; Awasthia, S.K.; Liu, T.; Zhang, Z.Q.; Awasthi, M.K. Response of bamboo biochar amendment on volatile fatty acids accumulation reduction and humification during chicken manure composting. *Bioresour. Technol.* **2019**, *291*, 121845. [CrossRef] [PubMed]
32. Zhang, Y.C.; Yue, D.B.; Ma, H. Darkening mechanism and kinetics of humification process in catechol-Maillard system. *Chemosphere* **2015**, *130*, 40–45. [CrossRef]
33. Reddy, S.; Nagaraja, M.S.; Raj, T.P.; Patil, A.P.; Dhumgond, P. Elemental analysis, E4/E6 ratio and total acidity of soil humic and fulvic acids from different land use systems. *Ann. Plant Soil Res.* **2014**, *2*, 89–92.
34. Sun, Z.Y.; Wang, X.H.; Liu, C.; Fang, G.D.; Chu, L.G.; Gu, C.; Gao, J. Persistent free radicals from low-molecular-weight organic compounds enhance cross-coupling reactions and toxicity of anthracene on amorphous silica surfaces under light. *Environ. Sci. Technol.* **2021**, *55*, 3716–3726. [CrossRef] [PubMed]
35. Zhang, H.W.; Zhang, X.M.; Ding, L.; Gong, M.; Su, Y.; Wang, S.W. Polymerization and oxidation of phenols in supercritical water. *Water Sci. Technol.* **2019**, *80*, 4. [CrossRef]
36. Zhang, Z.T.; Yi, G.Y.; Li, P.; Wan, X.K.; Wang, X.D.; Zhang, C.X.; Zhang, Y.L.; Sun, Q. Electrochemical oxidation of hydroquinone using Eu-doped PbO_2 electrodes: Electrode characterization, influencing factors and degradation pathways. *J. Electroanal. Chem.* **2021**, *895*, 115493. [CrossRef]
37. Link, N.; Removski, N.; Yun, J.; Fleming, L.T.; Nizkorodov, S.A.; Bertram, A.K.; Al-Abadleh, H.A. Dust-catalyzed oxidative polymerization of catechol and its impacts on ice nucleation efficiency and optical properties. *ACS Earth Space Chem.* **2020**, *4*, 1127–1139. [CrossRef]
38. Gokturk, E.; Ocsoy, I.; Turac, E.; Sahmetlioglu, E. Horseradish peroxidase-based hybrid nanoflowers with enhanced catalytical activities for polymerization reactions of phenol derivatives. *Polym. Advan. Technol.* **2020**, *31*, 2371–2377. [CrossRef]
39. Velasco, L.F.; Fonseca, I.M.; Parra, J.B.; Lima, J.C.; Ania, C.O. Photochemical behaviour of activated carbons under UV irradiation. *Carbon* **2012**, *50*, 249–258. [CrossRef]
40. McNeill, K.; Canonica, S. Triplet state dissolved organic matter in aquatic photochemistry: Reaction mechanisms, substrate scope, and photophysical properties. *Environ. Sci. Process. Impacts* **2016**, *18*, 1381–1399. [CrossRef]
41. Khachatryan, L.; Vejerano, E.; Lomnicki, S.; Dellinger, B. Environmentally persistent free radicals (EPFRs). 1. Generation of reactive oxygen species in aqueous solutions. *Environ. Sci. Technol.* **2011**, *45*, 8559–8566. [CrossRef]
42. Yang, F.; Zhu, Q.; Gao, Y.; Jian, H.X.; Wang, C.P.; Sun, H.W. Effects of biochar-dissolved organic matter on the photodegradation of sulfamethoxazole and chloramphenicol in biochar solutions as revealed by oxygen reduction performances and free radicals. *Sci. Total Environ.* **2021**, *781*, 146807. [CrossRef]
43. Liu, F.H.; Zhu, K.C.; Wang, Z.Q.; Liu, J.B.; Ni, Z.; Ding, Y.Y.; Zhang, C.; Jia, H.Z. Production of reactive oxygen species and its role in mediating the abiotic transformation of organic carbon in sandy soil under vegetation restoration. *Carbon Res.* **2023**, *2*, 35. [CrossRef]
44. Zhang, Y. Theoretical Investigations of Reactions between Methanol and Several Free Radicals. Master's Thesis, Chongqing University, Chongqing, China, 2019.
45. Goutham, R.; Ramin, F. Role of persistent free radicals and lewis acid sites in visible-light-driven wet peroxide activation by solid acid biochar catalysts—A mechanistic study. *J. Hazard. Mater.* **2022**, *438*, 129514.
46. Jiang, H.Y.; Zhao, M.Z.; Hong, W.J.; Song, W.H.; Yan, S.W. Mechanistic and Kinetic consideration of the photochemically generated oxidative organic radicals in dissolved black carbon solutions under simulated solar Irradiation. *Environ. Sci. Technol.* **2024**, *58*, 760–770. [CrossRef] [PubMed]
47. Kim, S.H.; Matsubara, R.; Hayashi, M. Activated carbon-promoted dehydrogenation of hydroquinones to benzoquinones, naphthoquinones, and anthraquinones under molecular oxygen atmosphere. *J. Org. Chem.* **2019**, *5*, 2997–3003. [CrossRef]
48. Szabóa, V.; Mészáros, R.; Kónya, Z.; Kukovecz, Á.; Pálinkóa, I.; Sipos, P.; Szabados, M. Preparation and characterization of MnIn-layered double hydroxides (LDHs), extension of the synthesis to fabricate Mn M(III)-LDHs (M = Al, Sc, Cr, Fe, Ga), and the comparison of their photocatalytic and catalytic activities in the oxidation of hydroquinone. *J. Mol. Struct.* **2022**, *1*, 132966. [CrossRef]
49. Polyakov, V.; Evgeny, A.; Evgeny, L.; Roman, V. Molecular weight distribution of humic acids isolated from buried soils and Yedoma sediments. *Agronomy* **2023**, *13*, 1483. [CrossRef]

Disclaimer/Publisher's Note: The statements, opinions and data contained in all publications are solely those of the individual author(s) and contributor(s) and not of MDPI and/or the editor(s). MDPI and/or the editor(s) disclaim responsibility for any injury to people or property resulting from any ideas, methods, instructions or products referred to in the content.